Cellular/Molecular

Distinct Functions for Anterograde and Retrograde Sorting of SORLA in Amyloidogenic Processes in the Brain

Sonya B. Dumanis,[1]* Tilman Burgert,[1]* Safak Caglayan,[1] Annette Füchtbauer,[2] Ernst-Martin Füchtbauer,[2] Vanessa Schmidt,[1] and Thomas E. Willnow[1]

[1]Max Delbrueck Center for Molecular Medicine, D-13125 Berlin, Germany and [2]Department of Molecular Biology and Genetics, Aarhus University, DK-8000 Aarhus, Denmark

SORLA is a neuronal sorting receptor implicated both in sporadic and familial forms of AD. SORLA reduces the amyloidogenic burden by two mechanisms, either by rerouting internalized APP molecules from endosomes to the *trans*-Golgi network (TGN) to prevent proteolytic processing or by directing newly produced Aβ to lysosomes for catabolism. Studies in cell lines suggested that the interaction of SORLA with cytosolic adaptors retromer and GGA is required for receptor sorting to and from the TGN. However, the relevance of anterograde or retrograde trafficking for SORLA activity *in vivo* remained largely unexplored. Here, we generated mouse models expressing SORLA variants lacking binding sites for GGA or retromer to query this concept in the brain. Disruption of retromer binding resulted in a retrograde-sorting defect with accumulation of SORLA in endosomes and depletion from the TGN, and in an overall enhanced APP processing. In contrast, disruption of the GGA interaction did not impact APP processing but caused increased brain Aβ levels, a mechanism attributed to a defect in anterograde lysosomal targeting of Aβ. Our findings substantiated the significance of adaptor-mediated sorting for SORLA activities *in vivo*, and they uncovered that anterograde and retrograde sorting paths may serve discrete receptor functions in amyloidogenic processes.

Key words: **adaptors; APP processing; protein transport; retromer; SORLA; VPS10P domain receptors**

Significance Statement

SORLA is a sorting receptor that directs target proteins to distinct intracellular compartments in neurons. SORLA has been identified as a genetic risk factor for sporadic, but recently also for familial forms of AD. To confirm the relevance of SORLA sorting for AD processes in the brain, we generated mouse lines, which express trafficking mutants instead of the wild-type form of this receptor. Studying neuronal activities in these mutant mice, we dissected distinct trafficking routes for SORLA guided by two cytosolic adaptors termed GGA and retromer. We show that these sorting pathways serve discrete functions in control of amyloidogenic processes and may represent unique therapeutic targets to interfere with specific aspects of neurodegenerative processes in the diseased brain.

Introduction

Sorting protein-related receptor with A-type repeats (SORLA) is a member of the vacuolar protein sorting 10 protein (VPS10P) gene family, a group of neuronal sorting receptors that traffic target proteins between Golgi, plasma membrane, and endosomes. Earlier work identified central roles for VPS10P domain receptors in control of neuronal viability and function, and in the occurrence of neurodegenerative diseases (for review, see Willnow et al., 2008).

Concerning SORLA, association studies link variants of *SORL1* (the gene encoding SORLA) with increased risk of sporadic AD (Rogaeva et al., 2007; Naj et al., 2011). Additionally, recent findings suggest that *SORL1* mutations may also underlie autosomal dominant familial forms of this disease (Pottier et al., 2012). According to current models, SORLA impacts AD-related processes by two distinct mechanisms. It acts as a trafficking receptor for APP, which redirects APP from endosomes to the trans-Golgi network (TGN), reducing the extent of proteolytic breakdown into amyloidogenic and nonamyloidogenic products (Offe et al., 2006; Schmidt et al.,

Received Feb. 2, 2015; revised July 29, 2015; accepted Aug. 4, 2015.

Author contributions: S.B.D. and T.E.W. designed research; S.B.D., T.B., S.C., A.F., E.-M.F., and V.S. performed research; S.B.D., T.B., S.C., A.F., E.-M.F., V.S., and T.E.W. analyzed data; T.E.W. wrote the paper.

Studies were funded by grants from the Helmholtz-Association (iCEMED) and the Fritz-Thyssen-Foundation (to T.E.W.) and the Alexander-von-Humboldt Foundation (to S.B.D.). We are indebted to T. Pantzlaff and M. Schmeisser for expert technical assistance.

*S.B.D. and T.B. contributed equally to this work.

The authors declare no competing financial interests.

Correspondence should be addressed to Thomas E. Willnow, Max-Delbrueck-Center for Molecular Medicine, Robert-Roessle-Strasse 10, D-13125 Berlin, Germany. E-mail: willnow@mdc-berlin.de.

DOI:10.1523/JNEUROSCI.0427-15.2015

 0270-6474/15/3512703-11$15.00/0

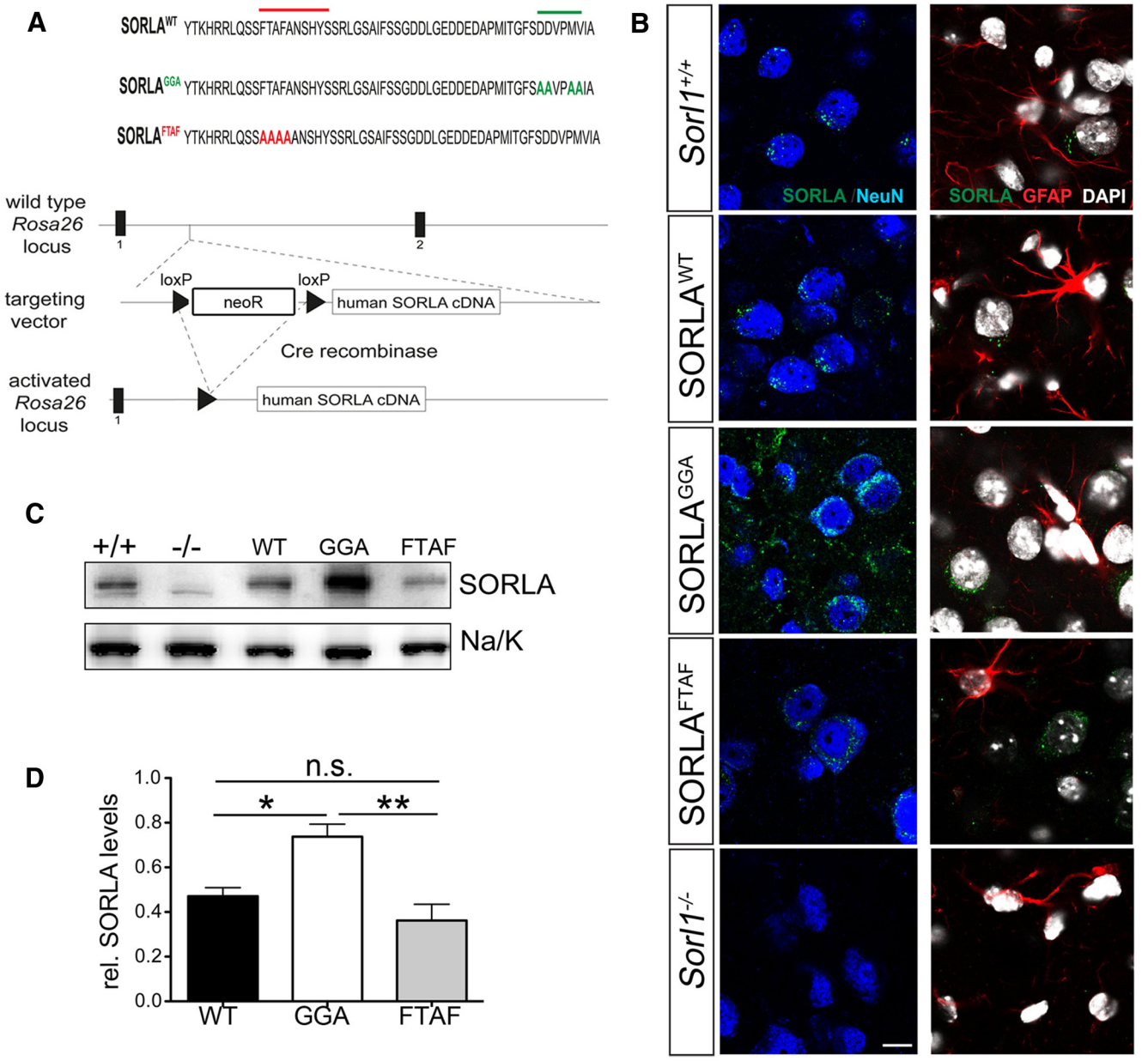

Figure 1. Mice expressing human SORLA variants. ***A***, Constructs encoding wild-type SORLA (SORLA ^{WT}) or receptor variants lacking the GGA (SORLA ^{GGA}) or retromer binding (SORLA ^{FTAF}) motifs for targeting the murine *Rosa26* locus are shown. Amino acid sequences of the cytoplasmic domains of the receptor variants with residues modified by mutagenesis in the GGA (green) and retromer (red) binding mutants are indicated. The scheme for introducing the targeting vectors between exons 1 and 2 (black squares) of *Rosa26* is given below. Removal of the *loxP*-flanked neomycin resistance cassette (neoR) enables transcription of the SORLA cDNAs from the *Rosa26* promoter (activated *Rosa26* locus). ***B***, Immunodetection of SORLA (green) in cortices of mice of the indicated genotypes. Sections were costained for the neuronal marker NeuN (blue; left) or astroglial marker GFAP (red) and DAPI (white; right). No immunoreactivity for SORLA is detectable in *Sorl1*$^{-/-}$ tissue (used as negative control). Scale bar, 10 μm. ***C***, ***D*** Western blot analysis (***C***) and quantification by densitometric scanning of replicate blots (***D***) documents increased levels for SORLA ^{GGA} compared with SORLA ^{WT} and SORLA ^{FTAF} in brain extracts ($n = 3$ animals/genotype; *$p < 0.05$, **$p < 0.01$, one-way ANOVA, Tukey *post hoc* analysis). Detection of Na/K ATPase (Na/K) served as loading control in ***C***.

2007). SORLA also acts as a sorting factor for Aβ, moving newly produced peptides to lysosomes for catabolism, further reducing the amyloidogenic burden (Caglayan et al., 2014).

Given the importance of SORLA-mediated protein sorting in AD, major attention has been focused on mechanisms governing receptor trafficking at the TGN. Two adaptors received particular attention, the Golgi-localizing, γ-adaptin ear homology domain ARF-interaction proteins (GGAs) and the retromer complex, both of which bind to the cytoplasmic tail of SORLA and are also genetically linked to AD (Small and Gandy, 2006; Wahle et al., 2006; Muhammad et al., 2008). Retromer is a pentameric adaptor complex involved in retrograde sorting of proteins from early endosomes to the TGN (Seaman, 2004; Small, 2008; Fjorback et al., 2012). GGAs mediate anterograde transport of cargo from the TGN to endosomes (Jacobsen et al., 2002; Herskowitz et al., 2012). In established cell lines, disruption of retromer or GGA binding to SORLA impairs trafficking of the receptor and alters APP processing fates (Schmidt et al., 2007; Herskowitz et al., 2012). However, direct proof that these sorting pathways are required for SORLA activity *in vivo* is lacking.

Here we generated mouse models expressing SORLA mutants defective in binding to retromer or GGAs, and we show that

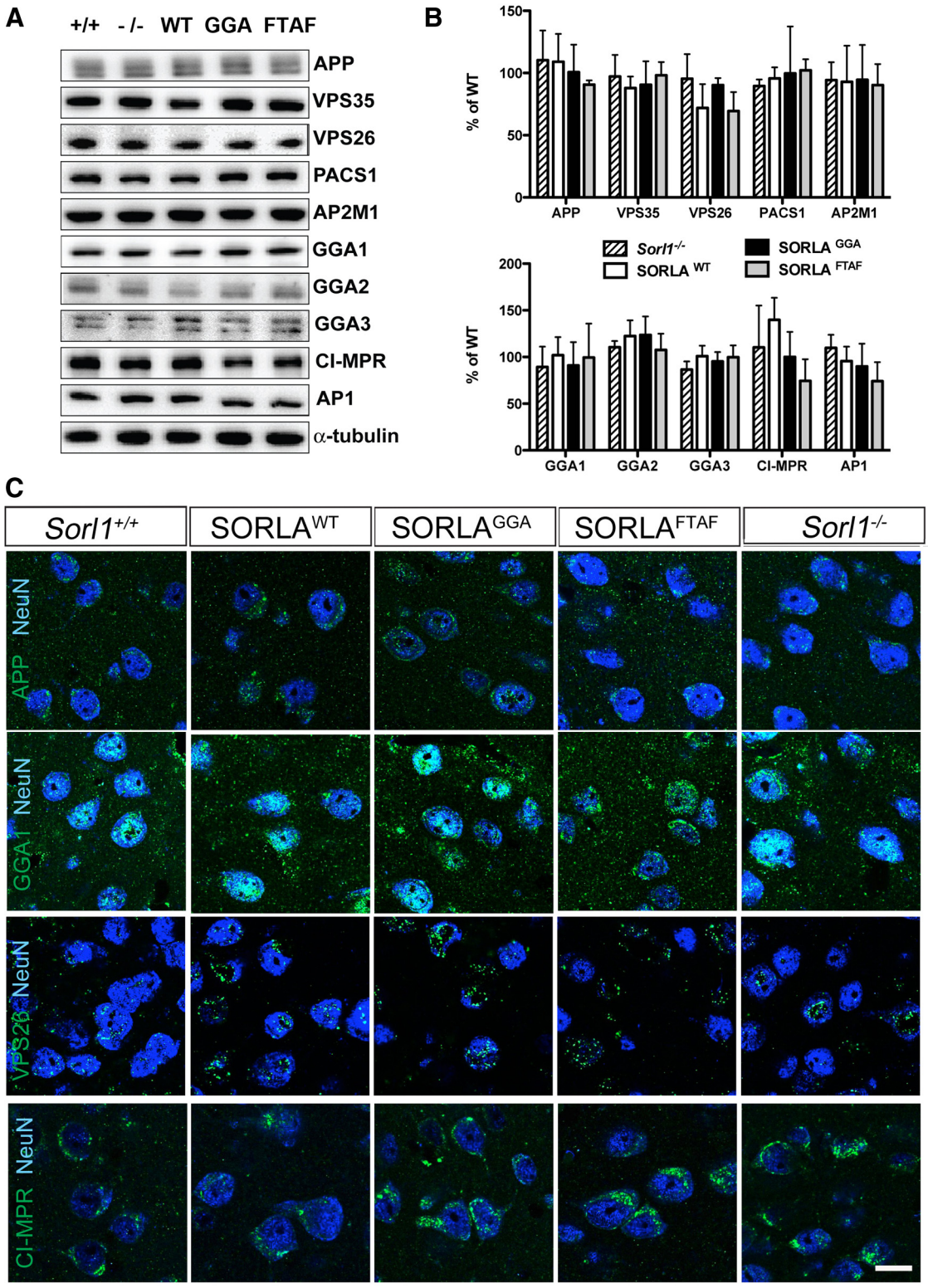

Figure 2. Characterization of proteins related to intracellular protein sorting. ***A***, Representative Western blots for proteins related to GGA and retromer activities in the cortices of mice of the various genotypes are shown. Detection of tubulin served as loading control. ***B***, Quantification of the Western blots in ***A*** revealed no significant differences in protein expression levels comparing the genotypes ($n = 3$ animals/genotype). ***C***, Immunodetection of neuronal marker NeuN (blue) and of proteins related to GGA and retromer activities (green) on cortical brain sections of mice of the indicated SORLA genotypes are shown. No discernable differences in neuronal expression patterns in the various genotypes are seen for APP (top row), GGA1 (second row), VPS26 (third row), or CI-MPR (bottom row) are seen. Scale bar, 15 μm.

disrupting these trafficking pathways differentially impacts SORLA activities *in vivo*. Lack of retromer binding impairs the APP sorting function of SORLA, resulting in an accumulation of the receptor in endosomes and in increased APP processing. In contrast, disrupting GGA binding decreases SORLA-dependent lysosomal targeting of Aβ, causing accumulation of the peptide in the brain. Our data document that SORLA-dependent trafficking of APP and Aβ requires distinct steps in anterograde and

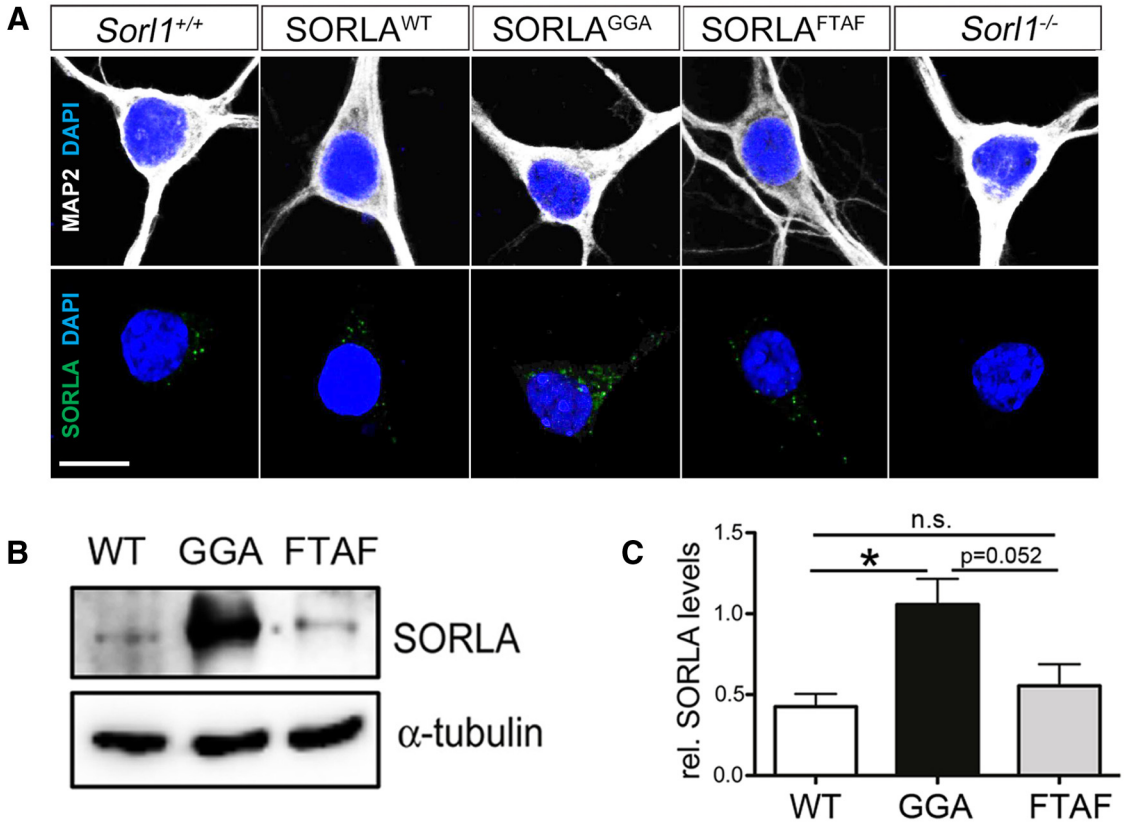

Figure 3. SORLA levels in primary neurons expressing wild-type and mutant receptor variants. ***A***, Representative images for primary hippocampal neurons (DIV 5) of the indicated genotypes stained for SORLA (green) and DAPI (blue; top), or for neuronal marker MAP2 (white) and DAPI (blue; bottom). Analysis of neuronal cultures from *Sorl1*$^{-/-}$ mice served as negative control. Scale bar, 10 μm. ***B***, ***C***, Levels of SORLA variants were tested by Western blotting of total cell lysates of primary neurons (***B***) and quantification by densitometric scanning of replicate blots (***C***). Levels of SORLA^{GGA} were increased compared with SORLA^{WT} and SORLA^{FTAF} ($n = 4$ per genotype; *$p < 0.05$, one-way ANOVA, Tukey *post hoc* analysis).

retrograde sorting, and that these pathways depend on the receptor interaction with GGAs and retromer, respectively.

Materials and Methods

Generation of mouse models. The generation of mice carrying a cDNA encoding wild-type human SORLA in the *Rosa26* locus (*Rosa26*^{TgSORLAwt}) has been described (Burgert et al., 2013). The same strategy was applied to generate mice carrying constructs for SORLA variants lacking GGA (*Rosa26*^{TgSORLAgga}) or retromer binding sites (*Rosa26*^{TgSORLftaf}; Fig. 1*A*). The constructs were introduced into the murine *Rosa26* gene locus using homologous recombination. Mice carrying the transgenes through their germline were crossed with the Cre deleter strain (Taconic) to remove a triple transcription stop site and to enable expression from the endogenous *Rosa26* promoter.

Analysis of brain tissue. Characterization of cortical brain tissues by fluorescence microscopy or Western blotting was performed using standard protocols. APP processing products were determined by multiplex assays (Meso Scale Discovery). Analyses were performed in female mice at 8–10 weeks of age. For differential extraction of Aβ, brain cortices were dissected and homogenized in ice-cold homogenization buffer (0.25 mM sucrose, 2 mM $MgCl_2$, and 20 mM Tris-HCl, pH 7.5). Following incubation for 20 min on ice, nuclei and cellular debris were removed by a centrifugation step (1000 × *g*, 10 min). The lysate was centrifuged (100,000 × *g*, 1 h), with the lysate becoming the soluble fraction. The pellet was resuspended in lysis buffer (1% NP-40, 1% Triton X-100, 50 mM Tris-HCl, pH 7.4, 300 mM NaCl) and centrifuged (100,000 × *g*, 1 h), with the new lysate labeled as the membrane bound fraction. This fraction was used for Western blot analysis. The pellet was subsequently resuspended in 70% formic acid, vortexed for 2 h, and centrifuged at 100,000 × *g* for 1 h. The resulting supernatant was neutralized in 1 M Tris and labeled the formic acid soluble fraction. All buffers were supplemented with protease inhibitor (05 892 791 001; Roche) and phosphatase inhibitors (78440; Thermo Scientific).

Hippocampal cell cultures. Primary neurons were generated from P1 mice and analyzed at 5 DIV (Rohe et al., 2008). Pearson's coefficient was determined using Fiji/ImageJ software. At least 20 neurons were imaged per condition. Experiments were replicated at least three times. Studies comparing SORLA^{GGA} with SORLA^{WT} and SORLA^{FTAF} with SORLA^{WT} strains were performed separately, therefore, statistically significant differences between mutant and wild-type lines in each group were evaluated using Student's *t* test. There was no statistically significant difference in the Pearson's coefficients of the respective SORLA^{WT} condition in both group sets.

Analysis of SH-SY5Y cells. For pulse chase experiments, SH-SY5Y cells stably overexpressing SORLA^{WT}, SORLA^{GGA}, or SORLA^{FTAF} were incubated in methionine-free medium for 60 min before adding 1.5 mM of the methionine analog L-azidohomoalanine (AHA; Invitrogen). After a 30 min pulse, the cells were chased for various time points and lysed. Using Click-It chemistry, an alkyne-biotin tag was added to AHA in the labeled proteins. Lysates were precipitated with protein A-Sepharose precoated with anti-SORLA IgG, and precipitates were subjected to SDS-PAGE and immunodetection with Streptavidin-HRP. Following densitometric scanning of replicate blots ($n = 8$ per condition), values were normalized to time point 0 of each experiment (set to 100%). A best-fit, one-phase exponential decay curve ($y = \text{Span}^{*}e^{-K*x} + \text{Plateau}$) was determined using GraphPad Prism software, with $t_{(1/2)} = 0.6932/K$. For the DAPT experiments, 5 μM DAPT [in the absence or presence of a lysosomal inhibitor cocktail (100 μM leupeptin, 10 μM pepstatin A, and 50 μM chloroquine)] was added to SH-SY5Y cells stably overexpressing APP and SORLA^{WT}, or APP and SORLA^{GGA} ($n = 9$ replicates). The decay of intracellular Aβ was determined as published previously (Caglayan et al., 2014).

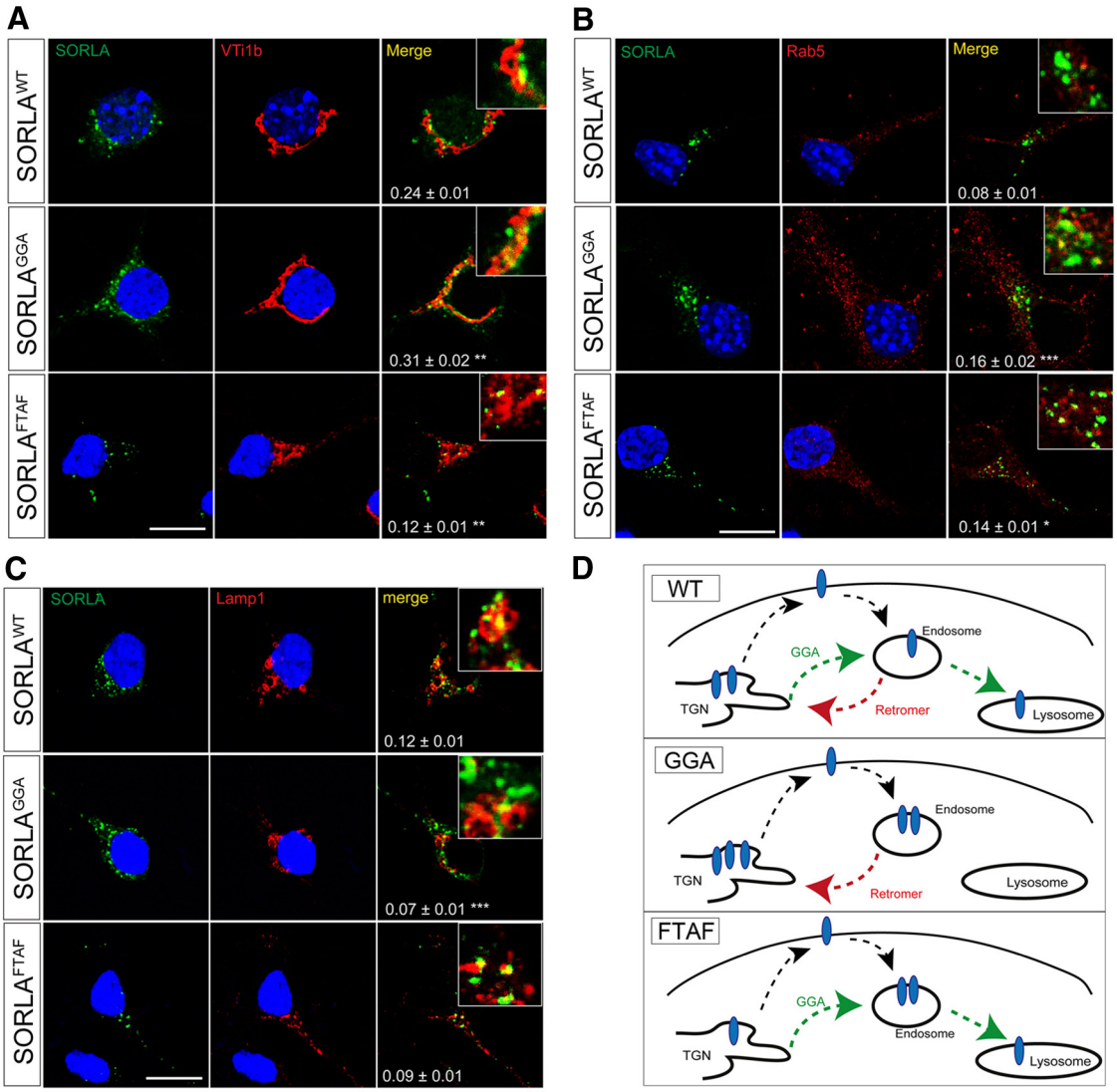

Figure 4. Aberrant trafficking of SORLA ^{GGA} and SORLA ^{FTAF} in hippocampal neurons. ***A–C***, Primary hippocampal neurons of the indicated genotypes stained for SORLA (green), DAPI (blue), and either VTi1b (red; ***A***), Rab5 (red; ***B***), or Lamp1 (red; ***C***). Pearson's coefficients are given in the merged parts. High-magnification insets indicate colocalization of SORLA with the respective marker. At least 20 neurons per genotype were imaged [$*p < 0.05$;$**p < 0.01$; $***p < 0.001$; Student's *t* test (as SORLA ^{WT} and SORLA ^{GGA} were performed separately from SORLA ^{WT} and SORLA ^{FTAF} experiments]. ***D***, Model of how SORLA localization changes in mutant receptor variants. SORLA ^{WT} is found predominantly in the TGN, but also in endosomes and lysosomes (top). Anterograde sorting from TGN to the endosomal/lysosomal compartments is mediated by GGAs (green arrow). Loss of this interaction results in SORLA ^{GGA} accumulation in the TGN and depletion from lysosomes (middle). Retrograde sorting of SORLA ^{WT} is mediated by retromer (red arrow). Loss of this interaction causes accumulation of SORLA ^{FTAF} in early endosomes but depletion from the TGN (bottom).

Results

To query the relevance of adaptors for SORLA trafficking *in vivo*, we generated two mouse models that express receptor variants defective in binding to GGA (SORLA ^{GGA}) or retromer (SORLA ^{FTAF}). We have applied this strategy before to produce mice expressing wild-type human SORLA (Burgert et al., 2013). In brief, we used PCR-based mutagenesis of the human SORLA cDNA to replace binding site residues for GGA (^{2207}DDVPMV^{2212}) or retromer (^{2169}FTAF^{2172}) in the cytoplasmic receptor domain by alanine residues (Fig. 1*A*). These modifications eliminate the ability of SORLA to interact with these adaptors in cultured cells (Schmidt et al., 2007; Fjorback et al., 2012). The cDNA constructs were introduced into the *Rosa26* locus of mice and activated by Cre-mediated recombination using the Cre deleter strain (Fig. 1*A*). Mice carrying the activated SORLA transgenes were crossed with animals having a targeted disruption of the endogenous SORLA locus (*Sorl1*$^{-/-}$; Andersen et al., 2005) to eliminate expression of the endogenous murine receptor. The corresponding mouse lines (*Rosa26*^{TgSORLAgga}, *Sorl1*$^{-/-}$) and (*Rosa26*^{TgSORLAftaf}, *Sorl1*$^{-/-}$) are referred to as SORLA ^{GGA} and SORLA ^{FTAF}, respectively. They were compared with(*Rosa26*^{TgSORLAwt}, *Sorl1*$^{-/-}$) animals (SORLA ^{WT}) expressing the human wild-type receptor in *Rosa26*.

Using immunohistology, we showed that all SORLA variants localized predominantly in the perinuclear region of neurons in the brain, similar to the pattern seen for the murine receptor in *Sorl1*$^{+/+}$ mice. No coexpression of the endogenous receptor or of transgenic SORLA variants with GFAP, a marker for astrocytes, was observed (Fig. 1*B*). This restricted expression of SORLA transgenes from *Rosa26* has been seen before and argued for cellular mechanisms that enable expression of this receptor in neurons but not in glia *in vivo* (Burgert et al., 2013; Caglayan et al., 2014). Surprisingly, SORLA ^{GGA} mice showed a stronger SORLA immunoreactivity compared with SORLA ^{WT} and SORLA ^{FTAF} (Fig. 1*B*). This notion was confirmed by Western blotting docu-

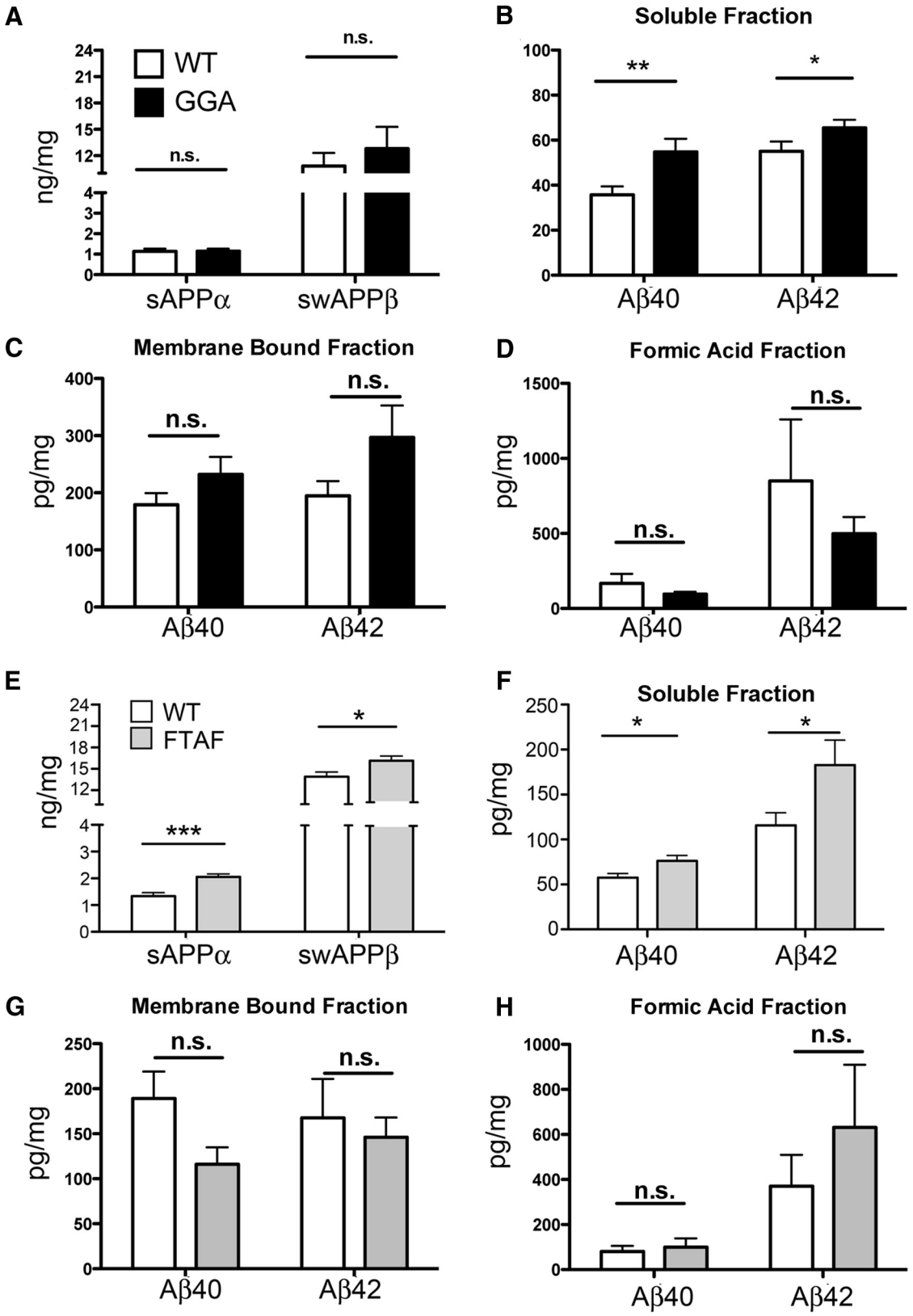

Figure 5. SORLA ^{GGA} and SORLA ^{FTAF} differentially impact amyloidogenic processing. SORLA ^{WT}, SORLA ^{GGA}, and SORLA ^{FTAF} mice were crossed with the 5xFAD line. Cortical lysates were collected from females at 8–10 weeks of age and analyzed as indicated. ***A–D***, Quantification by ELISA documents no changes in sAPPα and sAPPβ (swAPPβ). (***A***), but an increase in Aβ40 and Aβ42 levels (***B***) in SORLA ^{GGA} compared with SORLA ^{WT} mice in the soluble brain fraction ($n = 12$ animals/group). No difference in Aβ40 and Aβ42 levels was seen when the membrane bound (***C***) or formic acid soluble fractions (***D***) were analyzed ($n = 6–7$ animals/group). ***E–H***, ELISA documents increases in sAPPα and sAPPβ (***E***) and in Aβ40 and Aβ42 (***F***) in SORLA ^{FTAF} compared with SORLA ^{WT} animals ($n = 14–15$ animals/group) in the cytosolic brain fraction. Parallel experiments to ***E*** and ***F*** were performed, and quantification by ELISA documented no changes in Aβ40 and Aβ42 levels in SORLA ^{FTAF} compared with SORLA ^{WT} animals in the membrane bound (***G***) or formic acid soluble (***H***) fractions ($n = 7$ animals/group). Statistical analyses were performed using Student's *t* test (*$p < 0.05$; **$p < 0.01$; ***$p < 0.001$).

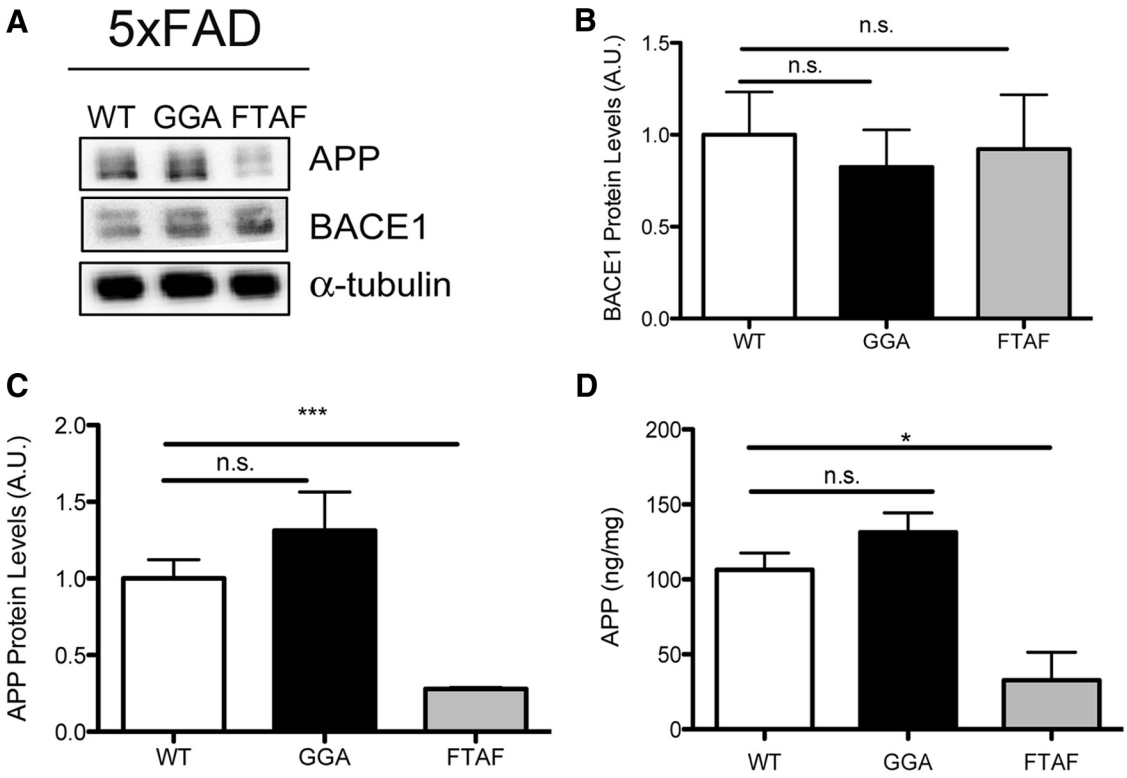

Figure 6. SORLA^{FTAF} mice have decreased levels of human APP. ***A***, Immunoblot analyses for APP and BACE1 in cortical brain extracts showing decreased levels of APP but not BACE1 in SORLA^{FTAF} mice. Tubulin served as loading control. ***B***, ***C***, Densitometric scanning of replicate Western blots (as exemplified in ***A***) confirms normal levels of BACE1 (***B***) but decreased levels of APP (***C***) in SORLA^{FTAF} compared with SORLA^{WT} and SORLA^{GGA} animals ($n = 3$/group; one-way ANOVA, Tukey *post hoc* analysis; ***$p < 0.001$). ***D***, ELISA substantiating decreased levels of APP in cortical extracts of SORLA^{FTAF} compared with SORLA^{WT} and SORLA^{GGA} animals ($n = 3$/group; one-way ANOVA, Tukey *post hoc* analysis; ***$p < 0.001$).

menting 56% increased levels of SORLA^{GGA} compared with the other receptor variants (Fig. 1*C*,*D*). Expression of the human SORLA variants did not alter brain levels (Fig. 2*A*,*B*) or cellular localization (Fig. 2*C*) of retromer subunits VPS26 and VPS35, of GGA1, GGA2, or GGA3, or of other SORLA adaptors, including PACS1, AP2 (μ-subunit), or AP1 (γ-adaptin; Fig. 2*A*,*B*). Also, the SORLA binding partners APP and cation-independent mannose-6 phosphate receptor (CI-MPR) showed comparable brain expression patterns in all genotypes (Fig. 2).

Next, we asked whether disruption of adaptor binding alters SORLA sorting in neurons as suggested by experiments in non-neuronal cell lines (Nielsen et al., 2007; Schmidt et al., 2007; Herskowitz et al., 2012). Consistent with our observation *in vivo* (Fig. 1*B*), all three SORLA variants localized to the perinuclear region in primary hippocampal neurons with expression of SORLA^{GGA} being increased compared with SORLA^{WT} and SORLA^{FTAF}. This increase was seen by immunocytochemistry (Fig. 3*A*) and by Western blotting (Fig. 3*B*,*C*). To test for neuronal protein sorting, we costained primary neurons from the various mouse lines for SORLA and the organelle markers Vti1b (TGN; Fig. 4*A*), Rab5 (early endosomes; Fig. 4*B*), or Lamp1 (lysosomes; Fig. 4*C*). Colocalization of SORLA with these markers was determined by the Pearson's coefficient. Consistent with the established pattern of endogenous SORLA, SORLA^{WT} localized mainly to the TGN, and to a lesser extent to early endosomes and lysosomes. In contrast, SORLA^{GGA} showed increased localization to the TGN and to early endosomes, but a loss from lysosomes. Immunosignals for SORLA^{FTAF} were increased in endosomes, but decreased in the TGN. Localization to lysosomes in SORLA^{FTAF} was not changed compared with SORLA^{WT}. These data confirmed the relevance of GGA and retromer interactions for SORLA sorting in neurons. Specifically, they suggested that loss of anterograde sorting in SORLA^{GGA} retains retrograde trafficking from early endosomes back to the TGN, bypassing lysosomal receptor targeting (Fig. 4*D*). In contrast, loss of retrograde sorting in SORLA^{FTAF} promotes the anterograde movement of receptors to endosomal compartments, depleting it from the TGN (Fig. 4*D*).

Having confirmed the necessity of retromer and GGA interactions for receptor sorting, we tested whether loss of these interactions impacts the activities of SORLA in amyloidogenic processes. To do so, we crossed SORLA^{WT}, SORLA^{GGA}, and SORLA^{FTAF} lines with the 5xFAD model of AD (Oakley et al., 2006). As quantified by ELISA, expression of SORLA^{GGA} resulted in an increase in Aβ40 and Aβ42, but not in soluble APPα and APPβ (sAPPα and sAPPβ), compared with SORLA^{WT} (Fig. 5*A*,*B*). The increase in Aβ40 and Aβ42 levels was specific for the soluble fraction of the peptides (Fig. 5*B*) and not seen for the membrane bound (Fig. 5*C*) or the formic acid soluble (Fig. 5*D*) fractions that represent different forms of Aβ aggregates. In SORLA^{FTAF}, levels of all APP processing products, including sAPPα and sAPPβ (Fig. 5*E*) and Aβ40 and Aβ42 (Fig. 5*F*), were elevated. Similar to what had been seen for SORLA^{GGA}, levels of Aβ40 and Aβ42 were significantly elevated in the soluble (Fig. 5*F*) but not in the membrane bound (Fig. 5G) or the formic acid soluble (Fig. 5*H*) fractions. The observation that the SORLA mutants primarily impact soluble Aβ species is in line with a role for this receptor in controlling proximal steps in Aβ production and catabolism. The above data suggested that loss of retromer interaction blocked the ability of SORLA to protect APP from proteolytic breakdown while loss of GGA interaction abrogated its activity to cause lysosomal catabolism of Aβ but did not impact

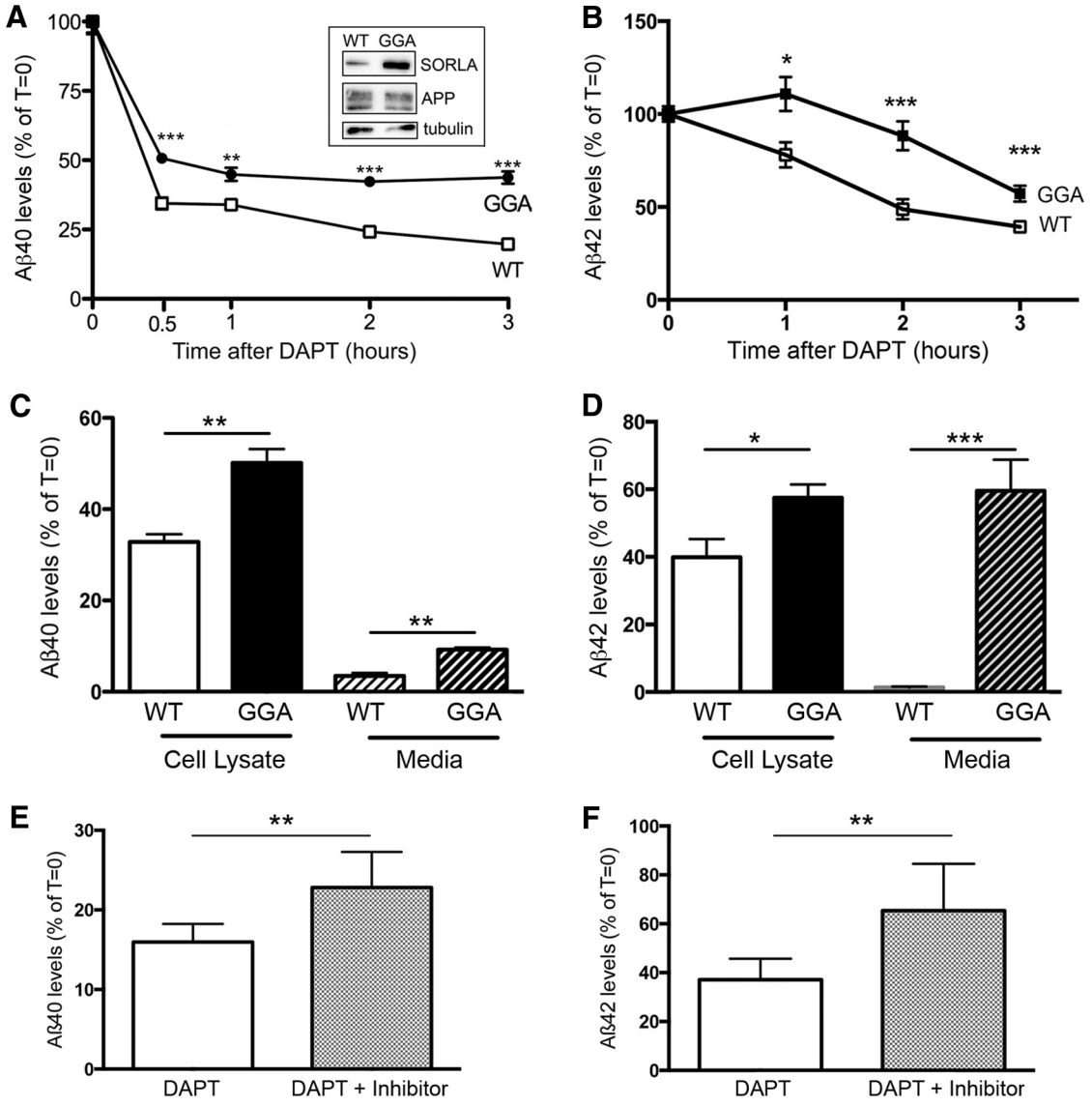

Figure 7. Impaired ability of SORLA^{GGA} to mediate lysosomal catabolism of Aβ peptides. ***A***, ***B***, SH-SY5Y cells overexpressing human APP^{695} together with SORLA^{WT} or SORLA^{GGA} were treated with 5 μM DAPT. At the indicated time points, the levels of intracellular Aβ40 (***A***) and Aβ42 (***B***) were determined by ELISA. Data represent the mean $\pm$ SEM of nine replicates expressed as percentage of time point 0 (set to 100%). Where no error bars are visible, they are smaller than the actual symbol shown. The inset in ***A*** documents expression of SORLA and APP in the cell extracts by Western blotting. ***C***, ***D***, Levels of Aβ40 (***C***) and Aβ42 (***D***) are increased in the cell lysate and the cell media of SORLA^{GGA} compared with SORLA^{WT} cells. Cells were treated with 5 μM DAPT for 3 h, and Aβ levels normalized to levels at time point 0 ($n = 3$ replicates). ***E***, ***F***, SORLA^{WT} cells were treated with 5 μM DAPT in the absence or presence of 100 μM leupeptin, 10 μM pepstatin A, and 50 μM chloroquine (DAPT + Inhibitor). Levels of Aβ40 (***E***) and Aβ42 (***F***) in the cell lysate were determined after 3 h and normalized to levels at time point 0 ($n = 6$ replicates). Application of the lysosomal inhibitor cocktail reduced catabolism of Aβ40 and Aβ42 compared with the DAPT only condition. Student's *t* test (*$p < 0.05$; **$p < 0.01$; ***$p < 0.001$).

APP processing. In line with these conclusions, levels of full-length human APP were reduced in SORLA^{FTAF} compared with SORLA^{WT} and SORLA^{GGA} indicating enhanced proteolytic breakdown of APP when retrograde sorting was blocked (Fig. 6*A*,*C*,*D*). The expression levels of BACE1 were not impacted by SORLA^{FTAF} or SORLA^{GGA} (Fig. 6*A*,*B*).

The loss of SORLA's ability to mediate lysosomal catabolism of Aβ, when GGA interaction was blocked, was confirmed in further cell experiments. Thus we generated SH-SY5Y cell lines overexpressing human APP^{695} and either SORLA^{WT} or SORLA^{GGA}. Similar to the situation in brain extracts (Fig. 1*D*) and primary neurons (Fig. 3*C*), the levels of SORLA^{GGA} in SH-SY5Y were significantly increased compared with SORLA^{WT}. In contrast, APP levels were unchanged, indicating normal rates of processing (Fig. 7*A*, inset). To study the intracellular catabolism of Aβ peptides, both cell lines were treated with the γ-secretase inhibitor DAPT to block *de novo* production of Aβ. Subsequently, the turnover of intracellular Aβ40 and Aβ42 was determined in cell extracts as published previously (Caglayan et al., 2014). In line with an impaired cellular catabolism, intracellular levels of Aβ40 and Aβ42 decreased slower in SY5Y-GGA compared with SY5Y-WT cells (Fig. 7*A*,*B*). Slower decline of Aβ levels in SY5Y-GGA cells was not from impaired secretion of the peptides, as Aβ40 and Aβ42 levels were higher in this cell line both in the cell lysates and in the cell medium after 3 h of DAPT treatment (Fig. 7*C*,*D*). This finding argued for an impaired intracellular catabolism of nascent Aβ peptides in SY5Y-GGA cells that resulted in intracellular accumulation and, consequently, enhanced release of the peptides. To substantiate the involvement of lysosomal pathways in the turnover Aβ in cells express-

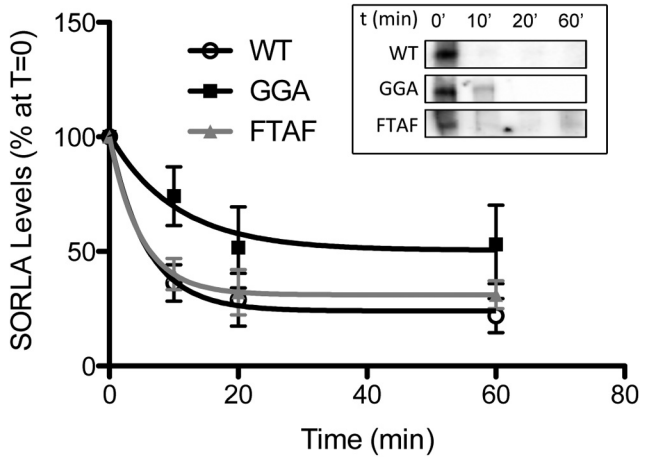

Figure 8. Prolonged half-life of SORLA^{GGA} compared with other receptor variants. Pulse-chase experiments were performed in SH-SY5Y cells stably transfected with SORLA^{WT}, SORLA^{GGA}, or SORLA^{FTAF}, and the amount of metabolically labeled SORLA at the chase time points determined by Western blotting (as exemplified in the inset). Following densitometric scanning of replicate blots, values were normalized to time point 0 of each experiment (set to 100%). A best-fit, one-phase exponential decay curve ($y = \text{Span}*e^{-K*x} + \text{Plateau}$) was determined using GraphPad Prism software, with $t_{(1/2)} = 0.6932/K$. Based on the curve fit, the protein half-life was $t_{(1/2)} = 3.97$ min for SORLA^{WT}, 3.43 min for SORLA^{FTAF}, but 7.17 min for SORLA^{GGA} ($n = 8$ replicates per condition). Data represent the mean ± SEM with the best-fit lines overlaid. Two-way ANOVA analysis (interaction between time and SORLA variant, n.s., time, $p < 0.001$, SORLA variant, $p < 0.05$) indicated that the SORLA^{GGA} cohort is significantly different from the other SORLA constructs.

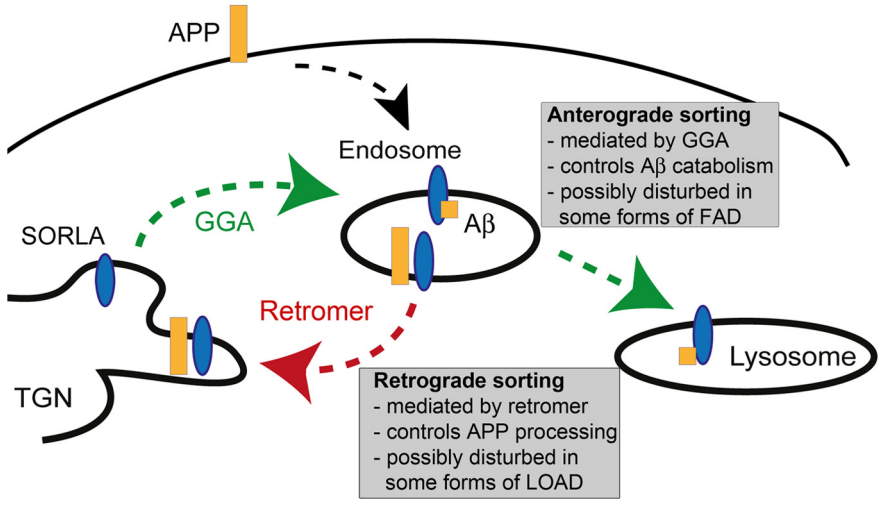

Figure 9. Model of SORLA trafficking pathways in amyloidogenic processes. GGAs mediate anterograde sorting of SORLA and impact SORLA-directed Aβ catabolism. An inherited mutation in *SORL1* that disrupts Aβ binding, abrogating SORLA-dependent lysosomal-catabolism of Aβ, is implicated in an autosomal-dominant familial form of AD (FAD). Retromer mediates retrograde sorting of SORLA, and disrupting this pathway reduces APP levels in the TGN and results in overall enhanced APP processing rate. Low levels of SORLA or retromer components in the brain are considered risk factors promoting late-onset forms of AD (LOAD).

ing SORLA, we treated SY5Y-WT cells with DAPT in the absence or presence of chloroquine, leupeptin, and pepstatin A. Combined application of these inhibitors of lysosomal proteolysis increased the intracellular levels of Aβ40 and Aβ42 compared with SY5Y-WT treated with DAPT only (Fig. 7*E*,*F*).

Neuronal levels of SORLA^{GGA} were elevated compared with SORLA^{WT} and SORLA^{FTAF} (Fig. 1*D*, 3*C*), suggesting an increased half-life of SORLA^{GGA} because of the absence of lysosomal targeting. This hypothesis was substantiated by pulse-chase experiments in metabolically labeled SH-SY5Y cells that documented an increased half-life for SORLA^{GGA} ($t_{(1/2)} = 7.17$ min) compared with SORLA^{WT} ($t_{(1/2)} = 3.97$) and SORLA^{FTAF} ($t_{(1/2)} = 3.43$ min; $p < 0.05$ for SORLA variant, two-way ANOVA; Fig. 8), and further supported GGA-mediated anterograde sorting of SORLA (and its cargo Aβ) to lysosomes.

Discussion

Considerable evidence implicates GGA and retromer in sorting defects in AD. Impaired activity of the adaptors is proposed to cause SORLA missorting and to enhance the amyloidogenic burden in sporadic AD (Wahle et al., 2006; Tesco et al., 2007; Muhammad et al., 2008). However, GGA and retromer also bind other cargo relevant to AD, including β-secretase (He et al., 2005; Wahle et al., 2005) or the related sorting receptors sortilin (Petersen et al., 1997; Nielsen et al., 2001) and SORCS1 (Lane et al., 2010), complicating the validation of this hypothesis. Using tailored mouse models expressing SORLA variants unable to bind GGA or retromer, we now document the functional interaction of SORLA with retromer and GGA in neurons in the brain. Levels of expression of other components of the neuronal sorting machinery or of alternative adaptor cargo were not impacted in these models. Our findings not only substantiated the relevance of SORLA and adaptor interaction *in vivo*, but also uncovered that anterograde and retrograde sorting pathways support discrete receptor activities relevant to AD.

Retromer emerges as a key player in sorting of proteins important for neuronal functions (Seaman, 2005; Small and Gandy, 2006; Muhammad et al., 2008; Siegenthaler and Rajendran, 2012). Dysfunction of this adaptor complex is seen in AD and PD (Small et al., 2005; Zavodszky et al., 2014). Binding of SORLA is mediated by the retromer subunit VPS26 (Fjorback et al., 2012), and disruption of this interaction causes altered localization and processing of APP in cells (Schmidt et al., 2007). Also, inactivation of retromer subunits in flies or mice increases Aβ levels (Muhammad et al., 2008) whereas pharmacological stabilization of the adaptor complex decreases APP processing (Mecozzi et al., 2014). In our mouse model, deletion of the retromer binding site in SORLA^{FTAF} results in enhanced proteolytic breakdown of human APP as judged by the decreased levels of the precursor (Fig. 6) and a concomitant increase in all processing products (Fig. 5*E*,*F*) in the 5xFAD line. Accelerated loss of full-length APP was not obvious for the murine wild-type protein (Fig. 2*A*), likely because this APP species is less prone to amyloidogenic processing than the human mutant APP$^{Swe(K670N),Florida(I716V),London(V717I)}$ variant expressed in the 5xFAD line. In primary neurons, SORLA^{FTAF} is depleted from the TGN but accumulates in early endosomes (Fig. 4*D*) supporting a model in which retrograde sorting results in sequestration of SORLA and APP in the TGN, protecting APP from processing in the secretory compartments (amyloidogenic pathway) and at the cell surface (nonamyloidogenic pathway). An increase in all APP processing products is also seen when the expression of SORLA is moderately re-

duced by siRNA to levels observed in individuals with *SORL1* risk alleles (Schmidt et al., 2012). Jointly, these observations suggest that altered APP sorting is a likely cause of AD in sporadic cases associated with risk alleles encoding SORLA or retromer subunits. A shift of SORLA from the TGN to early endosomes, and enhanced APP processing, is also seen in mice expressing a SORLA variant lacking an acidic tail motif (Burgert et al., 2013). This motif serves as a binding site for AP1 and PACS1, two other adaptors implicated in retrograde sorting. Likely, several adaptor pathways serve a redundant function in retrograde sorting of SORLA/APP complexes, and more severe phenotypes may be expected with receptor variants lacking acidic and FTAF motifs.

Contrary to the situation with SORLA^{FTAF}, loss of interaction with GGAs results in accumulation of SORLA^{GGA} in the TGN and in early endosomes. Most likely, internalization of SORLA^{GGA} molecules from the cell surface provides a sufficient supply of receptors to endosomal compartments to sustain retrograde sorting of APP (Fig. 4*D*). In line with this assumption, overall processing of APP is not increased in the SORLA^{GGA} mouse (Fig. 5*A*). BACE, an alternative ligand for GGAs (Wahle et al., 2005), shows normal expression (Fig. 6*A*) and activity (Fig. 5*A*) in SORLA^{GGA} mice. Apparently, this function of GGAs is not impacted by the SORLA^{GGA} mutation. This led us to hypothesize that failure of SORLA to interact with GGAs disrupts anterograde movement of SORLA and Aβ to lysosomes, a route that regulates intracellular levels of receptor and ligand. Our studies in the human neuronal cell line SH-SY5Y cells (Fig. 7, 8) confirmed this hypothesis. We used SH-SY5Y cells in these experiments, as primary neuronal cultures generated too low a yield to successfully perform the pulse-chase pull-downs or to measure acute Aβ levels after DAPT treatment. However, our findings in SH-SY5Y cells are supported by studies in primary neuronal cultures demonstrating reduced SORLA^{GGA} localization in Lamp1-positive vesicles compared with SORLA^{WT} (Fig. 4*C*). The ability to direct Aβ to lysosomes is also blocked in a SORLA mutant identified in a family with an autosomal-dominant form of AD (Pottier et al., 2012). This mutation disrupts the binding site for Aβ in the VPS10P domain of SORLA (Caglayan et al., 2014; Kitago et al., 2015). Although human mutations in *GGA* or in the GGA binding domain of *SORL1* have not been reported yet, our findings suggest that defects in the anterograde sorting pathway for Aβ may underlie some early onset forms of AD not linked to APP or presenilin mutations.

In conclusion, our findings established the causal relationship in a neuronal protein sorting machinery composed of SORLA and adaptors GGA and retromer, and their relevance for amyloidogenic processes in the brain (Fig. 9). Further studies are likely to define additional regulatory components of this sorting pathway central to brain (patho)physiology.

References

Andersen OM, Reiche J, Schmidt V, Gotthardt M, Spoelgen R, Behlke J, von Arnim CA, Breiderhoff T, Jansen P, Wu X, Bales KR, Cappai R, Masters CL, Gliemann J, Mufson EJ, Hyman BT, Paul SM, Nykjaer A, Willnow TE (2005) Neuronal sorting protein-related receptor sorLA/LR11 regulates processing of the amyloid precursor protein. Proc Natl Acad Sci U S A 28:13461–13466. Medline

Burgert T, Schmidt V, Caglayan S, Lin F, Füchtbauer A, Füchtbauer EM, Nykjaer A, Carlo AS, Willnow TE (2013) SORLA-dependent and -independent functions for PACS1 in control of amyloidogenic processes. Mol Cell Biol 33:4308–4320. CrossRef Medline

Caglayan S, Takagi-Niidome S, Liao F, Carlo AS, Schmidt V, Burgert T, Kitago Y, Füchtbauer EM, Füchtbauer A, Holtzman DM, Takagi J, Willnow TE (2014) Lysosomal sorting of amyloid-beta by the SORLA receptor is impaired by a familial Alzheimer's disease mutation. Sci Transl Med 6:223ra20. CrossRef Medline

Fjorback AW, Seaman M, Gustafsen C, Mehmedbasic A, Gokool S, Wu C, Militz D, Schmidt V, Madsen P, Nyengaard JR, Willnow TE, Christensen EI, Mobley WB, Nykjaer A, Andersen OM (2012) Retromer binds the FANSHY sorting motif in SorLA to regulate Amyloid Precursor Protein sorting and processing. J Neurosci 32:1467–1480. CrossRef Medline

He X, Li F, Chang WP, Tang J (2005) GGA proteins mediate the recycling pathway of memapsin 2 (BACE). J Biol Chem 280:11696–11703. CrossRef Medline

Herskowitz JH, Offe K, Deshpande A, Kahn RA, Levey AI, Lah JJ (2012) GGA1-mediated endocytic traffic of LR11/SorLA alters APP intracellular distribution and amyloid-beta production. Mol Biol Cell 23:2645–2657. CrossRef Medline

Jacobsen L, Madsen P, Nielsen MS, Geraerts WP, Gliemann J, Smit AB, Petersen CM (2002) The sorLA cytoplasmic domain interacts with GGA1 and -2 and defines minimum requirements for GGA binding. FEBS Lett 511:155–158. CrossRef Medline

Kitago Y, Nagae M, Nakata Z, Yagi-Utsumi M, Takagi-Niidome S, Mihara E, Nogi T, Kato K, Takagi J (2015) Structural basis for amyloidogenic peptide recognition by sorLA. Nat Struct Mol Biol 22:199–206. CrossRef Medline

Lane RF, Raines SM, Steele JW, Ehrlich ME, Lah JA, Small SA, Tanzi RE, Attie AD, Gandy S (2010) Diabetes-associated SorCS1 regulates Alzheimer's amyloid-beta metabolism: evidence for involvement of SorL1 and the retromer complex. J Neurosci 30:13110–13115. CrossRef Medline

Mecozzi VJ, Berman DE, Simoes S, Vetanovetz C, Awal MR, Patel VM, Schneider RT, Petsko GA, Ringe D, Small SA (2014) Pharmacological chaperones stabilize retromer to limit APP processing. Nat Chem Biol 10:443–449. CrossRef Medline

Muhammad A, Flores I, Zhang H, Yu R, Staniszewski A, Planel E, Herman M, Ho L, Kreber R, Honig LS, Ganetzky B, Duff K, Arancio O, Small SA (2008) Retromer deficiency observed in Alzheimer's disease causes hippocampal dysfunction, neurodegeneration, and Abeta accumulation. Proc Natl Acad Sci U S A 105:7327–7332. CrossRef Medline

Naj AC, Jun G, Beecham GW, Wang LS, Vardarajan BN, Buros J, Gallins PJ, Buxbaum JD, Jarvik GP, Crane PK, Larson EB, Bird TD, Boeve BF, Graff-Radford NR, De Jager PL, Evans D, Schneider JA, Carrasquillo MM, Ertekin-Taner N, Younkin SG, et al. (2011) Common variants at MS4A4/MS4A6E, CD2AP, CD33 and EPHA1 are associated with late-onset Alzheimer's disease. Nat Genet 43:436–441. CrossRef Medline

Nielsen MS, Madsen P, Christensen EI, Nykjaer A, Gliemann J, Kasper D, Pohlmann R, Petersen CM (2001) The sortilin cytoplasmic tail conveys Golgi-endosome transport and binds the VHS domain of the GGA2 sorting protein. EMBO J 20:2180–2190. CrossRef Medline

Nielsen MS, Gustafsen C, Madsen P, Nyengaard JR, Hermey G, Bakke O, Mari M, Schu P, Pohlmann R, Dennes A, Petersen CM (2007) Sorting by the cytoplasmic domain of the amyloid precursor protein binding receptor SorLA. Mol Cell Biol 27:6842–6851. CrossRef Medline

Oakley H, Cole SL, Logan S, Maus E, Shao P, Craft J, Guillozet-Bongaarts A, Ohno M, Disterhoft J, Van Eldik L, Berry R, Vassar R (2006) Intraneuronal beta-amyloid aggregates, neurodegeneration, and neuron loss in transgenic mice with five familial Alzheimer's disease mutations: potential factors in amyloid plaque formation. J Neurosci 26:10129–10140. CrossRef Medline

Offe K, Dodson SE, Shoemaker JT, Fritz JJ, Gearing M, Levey AI, Lah JJ (2006) The lipoprotein receptor LR11 regulates amyloid beta production and amyloid precursor protein traffic in endosomal compartments. J Neurosci 26:1596–1603. CrossRef Medline

Petersen CM, Nielsen MS, Nykjaer A, Jacobsen L, Tommerup N, Rasmussen HH, Roigaard H, Gliemann J, Madsen P, Moestrup SK (1997) Molecular identification of a novel candidate sorting receptor purified from human brain by receptor-associated protein affinity chromatography. J Biol Chem 272:3599–3605. CrossRef Medline

Pottier C, Hannequin D, Coutant S, Rovelet-Lecrux A, Wallon D, Rousseau S, Legallic S, Paquet C, Bombois S, Pariente J, Thomas-Anterion C, Michon A, Croisile B, Etcharry-Bouyx F, Berr C, Dartigues JF, Amouyel P, Dauchel H, Boutoleau-Bretonnière C, Thauvin C, et al. (2012) High frequency of potentially pathogenic SORL1 mutations in autosomal dominant early-onset Alzheimer disease. Mol Psychiatry 17:875–879. CrossRef Medline

Rogaeva E, Meng Y, Lee JH, Gu Y, Kawarai T, Zou F, Katayama T, Baldwin CT, Cheng R, Hasegawa H, Chen F, Shibata N, Lunetta KL, Pardossi-Piquard R, Bohm C, Wakutani Y, Cupples LA, Cuenco KT, Green RC,

Pinessi L, et al. (2007) The neuronal sortilin-related receptor SORL1 is genetically associated with Alzheimer disease. Nat Genet 39:168–177. CrossRef Medline

Rohe M, Carlo AS, Breyhan H, Sporbert A, Militz D, Schmidt V, Wozny C, Harmeier A, Erdmann B, Bales KR, Wolf S, Kempermann G, Paul SM, Schmitz D, Bayer TA, Willnow TE, Andersen OM (2008) SORLA controls APP-dependent stimulation of ERK signaling and adult neurogenesis. J Biol Chem 283:14826–14834. CrossRef Medline

Schmidt V, Sporbert A, Rohe M, Reimer T, Rehm A, Andersen OM, Willnow TE (2007) SorLA/LR11 regulates processing of amyloid precursor protein via interaction with adaptors GGA and PACS-1. J Biol Chem 282: 32956–32964. CrossRef Medline

Schmidt V, Baum K, Lao A, Rateitschak K, Schmitz Y, Teichmann A, Wiesner B, Petersen CM, Nykjaer A, Wolf J, Wolkenhauer O, Willnow TE (2012) Quantitative modelling of amyloidogenic processing and its influence by SORLA in Alzheimer's disease. EMBO J 31:187–200. CrossRef Medline

Seaman MN (2004) Cargo-selective endosomal sorting for retrieval to the Golgi requires retromer. J Cell Biol 165:111–122. CrossRef Medline

Seaman MN (2005) Recycle your receptors with retromer. Trends Cell Biol 15:68–75. CrossRef Medline

Siegenthaler BM, Rajendran L (2012) Retromers in Alzheimer's disease. Neurodegener Dis 10:116–121. CrossRef Medline

Small SA (2008) Retromer sorting: a pathogenic pathway in late-onset Alzheimer disease. Arch Neurol 65:323–328. CrossRef Medline

Small SA, Gandy S (2006) Sorting through the cell biology of Alzheimer's disease: intracellular pathways to pathogenesis. Neuron 52:15–31. CrossRef Medline

Small SA, Kent K, Pierce A, Leung C, Kang MS, Okada H, Honig L, Vonsattel JP, Kim TW (2005) Model-guided microarray implicates the retromer complex in Alzheimer's disease. Ann Neurol 58:909–919. CrossRef Medline

Tesco G, Koh YH, Kang EL, Cameron AN, Das S, Sena-Esteves M, Hiltunen M, Yang SH, Zhong Z, Shen Y, Simpkins JW, Tanzi RE (2007) Depletion of GGA3 stabilizes BACE and enhances beta-secretase activity. Neuron 54:721–737. CrossRef Medline

Wahle T, Prager K, Raffler N, Haass C, Famulok M, Walter J (2005) GGA proteins regulate retrograde transport of BACE1 from endosomes to the trans-Golgi network. Mol Cell Neurosci 29:453–461. CrossRef Medline

Wahle T, Thal DR, Sastre M, Rentmeister A, Bogdanovic N, Famulok M, Heneka MT, Walter J (2006) GGA1 is expressed in the human brain and affects the generation of amyloid beta-peptide. J Neurosci 26:12838–12846. CrossRef Medline

Willnow TE, Petersen CM, Nykjaer A (2008) VPS10P-domain receptors—regulators of neuronal viability and function. Nat Rev Neurosci 9: 899–909. CrossRef Medline

Zavodszky E, Seaman MN, Moreau K, Jimenez-Sanchez M, Breusegem SY, Harbour ME, Rubinsztein DC (2014) Mutation in VPS35 associated with Parkinson's disease impairs WASH complex association and inhibits autophagy. Nat Commun 5:3828. CrossRef Medline